Acta Cryst. (1981). A**37**, 787–794

Three-Beam Effects in *Pendellösung* Fringes

BY R. HØIER AND A. AANESTAD*

Institutt for Røntgenteknikk, Universitetet i Trondheim-NTH, N-7034 Trondheim-NTH, Norway

(*Received* 18 *February* 1981; *accepted* 2 *April* 1981)

Abstract

The perturbations of standard two-beam *Pendellösung* fringes due to simultaneous excitation of an additional Bragg beam have been studied. For a qualitative understanding of the observed local changes in both fringe position and intensity, a plane-wave description has proved to be sufficient. Through three-beam calculations of Bloch-wave excitation coefficients it is found that the main intensity terms may be ascribed to the same four dispersion surface branches which are excited also in the corresponding two-beam case. The continuous variation observed in the fringe period and position is explained from the variation in the width of the dispersion surface gap. This gap varies with the sign and size of the deviation parameter of the simultaneously excited beam. For a given deviation parameter the gap width also depends on the sign of the product between the three structure factors involved. The resulting dependence of the fringe displacement on this sign may be utilized to determine the three-phase structure invariant experimentally.

Introduction

In conventional single-crystal X-ray diffraction experiments the observed intensities may be strongly influenced by effects due to simultaneous diffraction of several Bragg beams (Renninger, 1937). Such effects are as a rule not included in the standard theoretical description and care is therefore generally taken in the X-ray case to avoid many-beam situations experimentally.

It is well known, however, that structural information which is otherwise not obtainable may be extracted from experiments involving more than two beams. This has most clearly been demonstrated in the electron diffraction case where the application of dynamical many-beam effects has received considerable attention (see references in, for example, Terasaki, Watanabe & Gjønnes, 1979; Kambe & Molière, 1970). The possibility of determining a three-phase structure invariant from essentially absorption-independent three-beam effects was, for example, discussed by Kambe (1957) and Gjønnes & Høier (1969). Conclusions from the former paper were directly applied by Hart & Lang (1961) to interpret an observation of a three-beam effect in X-ray *Pendellösung* fringes. The general validity of the electron diffraction results in their case was not discussed, however, and no calculations were given.

Various papers exist on X-ray many-beam cases, *e.g.* Saccocio & Zajac (1965); Hildebrandt (1967); Joko & Fukuhara (1967); Ewald & Heno (1968); Katsnelson, Iveronova, Borodina & Runova (1975); Post, Chang & Huang (1977) and Post (1979). Comparisons between theory and experiments are relatively limited and in most cases focused on anomalous absorption effects. These may, however, be utilized to yield structure information in special cases, and Post (1977) has shown that the variation in anomalous absorption in a three-beam case may be used to determine a three-phase structure invariant.

Another type of experiment for which a plane wave many-beam description may be applicable on a qualitative scale is the *Pendellösung* case. This essentially absorption-independent effect has been studied in detail experimentally as well as theoretically in the two-beam case with both plane-wave and spherical-wave theory (*e.g.* Kato, 1968*a*,*b*; Tanemura & Kato, 1972; Aldred & Hart, 1973*a*,*b*; Wada & Kato, 1977). In both types of theoretical description it is clear that the fringe period directly reflects the minimum distance between the dispersion surface branches. If this gap is perturbed due to a many-beam interaction the fringe distance may be expected to change as well.

The development of methods to extract structural information from observed many-beam diffraction effects depends on a detailed theoretical understanding of the effects utilized. We have in this work aimed at obtaining a qualitative description of an observed three-beam effect in *Pendellösung* fringes with plane-wave theory which for not too thin crystals is known to give the fringe distance correctly. The variations in the Bloch-wave excitation coefficients and the beam intensities have been studied in detail, and one has focused on the interpretation of the observed effects by means of the dispersion surface. Some preliminary results have

* Present address: SINTEF, Avd. 16-Mekanisk teknologi, N-7034 Trondheim-NTH, Norway.

0567-7394/81/060787-08$01.00

been given previously (Høier, Ekrann & Aanestad, 1978).

Theory

The solution of Maxwell's equations in a medium with a periodic susceptibility has the Bloch form (*e.g.* James, 1963; Azaroff, Kaplow, Kato, Weiss, Wilson & Young, 1974):

$$\mathbf{D}^j = \sum_h \mathbf{D}_h^j \exp\,[2\pi i(vt - \mathbf{K}_h^j.\mathbf{r})]. \qquad (1)$$

The crystal wave vector for solution j is written

$$\mathbf{K}_h^j = \mathbf{K}_0 + \mathbf{h} - \boldsymbol{\Gamma}^j. \qquad (2)$$

The quantity $\boldsymbol{\Gamma}^j$ is introduced as a measure of the *Anpassung*. $\boldsymbol{\Gamma}^j$, which is antiparallel to the surface normal, as shown in Fig. 1, depends on the deviation from the Bragg condition given by the excitation error $\mathbf{s}_h$. Both $\boldsymbol{\Gamma}^j$ and $\mathbf{s}_h$ are taken to be positive in the figure. In Fig. 1 and below we shall only discuss many-beam cases where the entrance surface normal is parallel to the zone axis defined by the diffracting planes.

The wave field is decomposed into two orthogonal directions determined by the unit vectors $\boldsymbol{\sigma}$ and $\boldsymbol{\pi}$, *e.g.*

$$\mathbf{D}_h^j = D_{h\sigma}^j \boldsymbol{\sigma}_h + D_{h\pi}^j \boldsymbol{\pi}_h, \qquad (3)$$

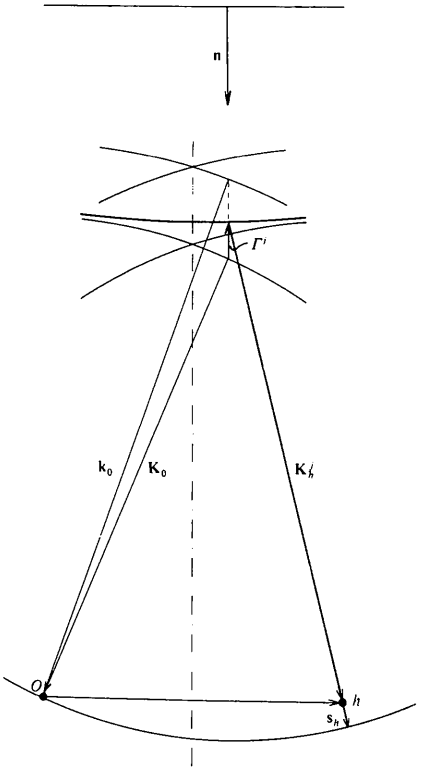

Fig. 1. Two-beam dispersion-surface construction with definition of $\mathbf{s}_h$ and $\boldsymbol{\Gamma}^j$.

where $\boldsymbol{\sigma}_h \times \boldsymbol{\pi}_h = \hat{\mathbf{K}}_h$. By introducing these components in the fundamental equation the following eigenvalue problem is obtained (*e.g.* Saccocio & Zajac, 1965):

$$\begin{bmatrix} -\Gamma_s & 0 & \cdots & \psi_{-h}\boldsymbol{\sigma}_0.\boldsymbol{\sigma}_h & \psi_{-h}\boldsymbol{\sigma}_0.\boldsymbol{\pi}_h & \cdots \\ 0 & -\Gamma_s & \cdots & \psi_{-h}\boldsymbol{\pi}_0.\boldsymbol{\sigma}_h & \psi_{-h}\boldsymbol{\pi}_0.\boldsymbol{\pi}_h & \cdots \\ \vdots & \vdots & & \vdots & \vdots & \\ & & & \psi_{g-h}\boldsymbol{\sigma}_g.\boldsymbol{\sigma}_h & \psi_{g-h}\boldsymbol{\sigma}_g.\boldsymbol{\pi}_h & \cdots \\ & & & \psi_{g-h}\boldsymbol{\pi}_g.\boldsymbol{\sigma}_h & \psi_{g-h}\boldsymbol{\pi}_g.\boldsymbol{\pi}_h & \cdots \\ & & & \vdots & \vdots & \\ \psi_h\boldsymbol{\sigma}_h.\boldsymbol{\sigma}_0 & \psi_h\boldsymbol{\sigma}_h.\boldsymbol{\pi}_0 & \cdots & s_h - \Gamma_s & 0 & \cdots \\ \vdots & \vdots & & \vdots & \vdots & \end{bmatrix} \cdot \begin{bmatrix} D_{0\sigma} \\ D_{0\pi} \\ \vdots \\ D_{g\sigma} \\ D_{g\pi} \\ \vdots \\ D_{h\sigma} \\ D_{h\pi} \end{bmatrix} = 0. \qquad (4)$$

In this equation Γ_s is the component of $\boldsymbol{\Gamma}$ along the wave vectors. We have further introduced the quantity

$$\psi_h = -\frac{r_e}{2K\pi V} F_h, \qquad (5)$$

where r_e is the classical electron radius, V is the unit-cell volume and F_h is the structure factor. Absorption may be ascribed to the imaginary part of ψ_h which in general may be written

$$\psi_h = \psi_h' + i\psi_h''. \qquad (6)$$

In (4) this leads to an additional term $i\psi_0''$ in all the diagonal elements and terms of the type $i\psi_{g-h}''\,\boldsymbol{\sigma}_g.\boldsymbol{\pi}_h$ in all the off-diagonal elements. The wave vector given by (2) is thus generally complex through the imaginary component $\Gamma^{j\prime\prime}$ of the eigenvalue.

For each incident beam direction (4) may now be solved for the n-beam case, analytically or numerically, to give the $2n$ *orthonormalized* solutions

$$\mathbf{D}^j = \sum_h (D_{h\sigma}^j \boldsymbol{\sigma}_h + D_{h\pi}^j \boldsymbol{\pi}_h) \exp\,[2\pi i(vt - \mathbf{K}_h^j.\mathbf{r})]. \qquad (7)$$

The actual crystal wave fields are found from $\mathbf{D}^j$ by introducing the expansion coefficients α^j. With $\boldsymbol{\tau}$ as a vector in the entrance surface, the continuity condition at the entrance surface is written

$$E_{\mathrm{in},\sigma}\,\boldsymbol{\sigma}_{\mathrm{in}} \exp\,(-2\pi i\mathbf{k}.\boldsymbol{\tau}) = \sum_j \alpha^j(\sigma) \sum_h \mathbf{D}_h^j \times \exp\,(-2\pi i\mathbf{K}_h^j.\boldsymbol{\tau}). \qquad (8)$$

This equation refers to the σ polarization state of the incident beam, $E_{\mathrm{in},\sigma}\,\boldsymbol{\sigma}_{\mathrm{in}}$. The π state of the incident beam leads independently to a corresponding equation.

$\alpha^j(\sigma)$ is determined from (8) by multiplication with the factor $\mathbf{D}^{i*}$ followed by an integration over the surface. Utilizing the orthonormality of the eigen-

solutions one obtains, provided $\boldsymbol{\sigma}_{\text{in}}$ is taken to be parallel to $\boldsymbol{\sigma}_0$,

$$\alpha^j(\sigma) = E_{\text{in},\sigma}\, D^{j*}_{0\sigma} \tag{9a}$$

and correspondingly for the π state of the incident beam

$$\alpha^j(\pi) = E_{\text{in},\pi}\, D^{j*}_{0\pi}. \tag{9b}$$

For the **h** component of the field due to the σ state of the incident beam we thus obtain

$$\mathbf{D}_h(\sigma) = E_{\text{in},\sigma} \sum_j D^{j*}_{0\sigma}(D^j_{h\sigma}\,\boldsymbol{\sigma}_h + D^j_{h\pi}\,\boldsymbol{\pi}_h) \times \exp[2\pi i(\nu t - \mathbf{K}^j_h.\mathbf{r})]. \tag{10}$$

The total intensity is hence

$$I_h = I_h(\sigma) + I_h(\pi), \tag{11}$$

where, for example, the σ component is

$$I_h(\sigma) = |\mathbf{D}_h(\sigma)|^2 = \tfrac{1}{2}|\sum_j D^{j*}_{0\sigma}(D^j_{h\sigma}\,\boldsymbol{\sigma}_h + D^j_{h\pi}\,\boldsymbol{\pi}_h) \times \exp(-2\pi i \Gamma^{j\prime} z)\exp(-\mu^j z)|^2. \tag{12}$$

As the incident beam is assumed to be unpolarized the field components on average have the values

$$\langle |E_{\text{in},\sigma}|^2\rangle = \langle |E_{\text{in},\pi}|^2\rangle = \tfrac{1}{2}.$$

Further, $\Gamma^{j\prime}$ and $\Gamma^{j\prime\prime}$ are the real and imaginary parts of the eigenvalue, respectively, such that the Bloch-wave amplitude absorption parameter can be written

$$\mu^j = -2\pi\Gamma^{j\prime\prime}. \tag{13}$$

For each polarization direction the intensity expression can be divided into a non-oscillating term, *e.g.*

$$I^{\text{non}}_h(\sigma) = \tfrac{1}{2}\sum_j |D^j_{0\sigma}|^2(|D^j_{h\sigma}|^2 + |D^j_{h\pi}|^2)\exp(-2\mu^j z), \tag{14}$$

and a term which oscillates with the crystal thickness z, *i.e.*

$$I^{\text{osc}}_h(\sigma) = \sum_{i,j} A^{ij}_{0h} \cos[2\pi(\Gamma^{i\prime} - \Gamma^{j\prime})z] \times \exp[-(\mu^i + \mu^j)z]. \tag{15}$$

In (15) we have introduced the quantity

$$A^{ij}_{0h} = D^i_{0\sigma}\, D^{j*}_{0\sigma}(D^{i*}_{h\sigma}\, D^j_{h\sigma} + D^{i*}_{h\pi}\, D^j_{h\pi}), \tag{16}$$

which is in general complex. The imaginary part is negligible, however, when $\psi''_h \ll \psi'_h$, and the phase shift which follows is not included in (15).

In (14) the contribution to each beam direction **h** depends on the factor $|D^j_{0\sigma}|^2$. This is an important factor which weighs the contribution to the average intensity from each dispersion surface branch. By analogy with the similar factor in many-beam electron diffraction theory (see *e.g.* Høier, 1973), we call this factor the Bloch-wave intensity excitation coefficient, $\varepsilon^j(\sigma)$. For the independent σ and π states of the incident beam we get respectively

$$\varepsilon^j(\sigma) = \frac{|\alpha^j(\sigma)|^2}{|E_{\text{in},\sigma}|^2} = |D^j_{0\sigma}|^2 \tag{17a}$$

and

$$\varepsilon^j(\pi) = \frac{|\alpha^j(\pi)|^2}{|E_{\text{in},\pi}|^2} = |D^j_{0\pi}|^2. \tag{17b}$$

Calculations

All the calculations presented below refer to the three-beam case shown in Fig. 2. The crystal is a Si wedge and characteristic Mo radiation is assumed. To determine the generally complex eigensystem from (4) we have used an algorithm described by Peters & Wilkinson (1970).

Each calculated value of the beam intensity corresponds to one particular incident beam direction, *i.e.* to one particular set of excitation errors s_g. Further, all s_g depend linearly on the single parameter ξ which is the distance from the exact three-beam condition to the tail of $\mathbf{K}_0$ projected on the reciprocal plane considered, *i.e.* in the present case

$$s_g = \boldsymbol{\xi}.\mathbf{g}/|\mathbf{K}|$$
$$s_h = 0, \tag{18}$$

as $\boldsymbol{\xi}$ is assumed to be parallel to the line Ag in Fig. 2. The calculated results are shown as functions of ξ, and the unit for ξ is in all figures taken to be 10^{-6} Å^{-1} corresponding to an angular deviation from the $0\bar{2}2$ Bragg angle of 0·13″ of arc.

From the direction of $\boldsymbol{\xi}$ chosen it follows that four of the six values of Γ calculated are associated with the 000, $2\bar{2}0$ two-beam dispersion surface gap. Only the

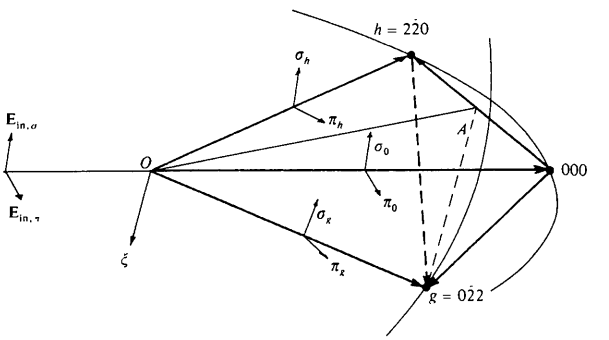

Fig. 2. Three-beam case with the polarization directions chosen. ξ parallel to Ag.

intensity variations along the $2\bar{2}0$ net planes within the Borrmann fan are hence theoretically predicted. These variations determine the observed *Pendellösung* period far from the three-beam condition. It is assumed that the section through the dispersion surface for $s_h = 0$ is the important one close to the three-beam condition as well.

In Fig. 3 the calculated value, Γ_ξ^j, of the real part of the eigenvalue above the ξ plane is shown as a function of ξ. (The ξ plane passes through O normal to the zone axis in Fig. 2.) The branches are numbered according to decreasing values of Γ^j for $\xi < 0$. The corresponding numbering for $\xi > 0$ follows from the symmetry of the eigenvector components. At $\xi = 0$ the solution shows one triple- and one double-degenerate root as expected (Joko & Fukuhara, 1967). Of particular interest here is the distance between the branches 1, 2, 3 and 4 for $\xi < 0$ and 1, 4, 5 and 6 for $\xi > 0$. The limiting values for large $|\xi|$ correspond to the values of the 000, $2\bar{2}0$ two-beam gap.

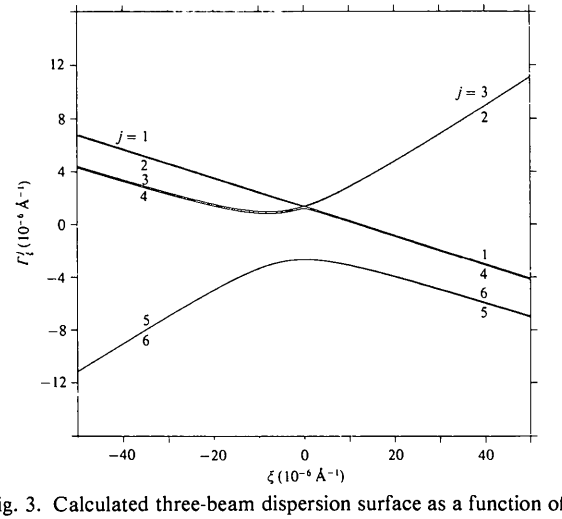

Fig. 3. Calculated three-beam dispersion surface as a function of ξ. $F_h F_{-g} F_{g-h} > 0$.

A section through the calculated absorption surface is shown in Fig. 4 where the Bloch-wave amplitude absorption coefficient, $\mu^j = -2\pi\Gamma^{j\prime\prime}$, is plotted as a function of ξ. For large positive and negative values of ξ the two-beam values are approached for the branches 1, 4, 5, 6 and 1, 2, 3, 4, respectively. The limiting value for the branches 2 and 3 for positive and 5 and 6 for negative values of ξ is for large $|\xi|$ equal to the average value of the amplitude absorption coefficient. Three branches are seen to have the same minimum value at $\xi = 0$ corresponding to the triple-degenerate root in Fig. 3.

The branches which will represent the main contribution to the intensity are found from the calculated excitation coefficients shown in Figs. 5 and 6. Apart from within a length of approximately $\xi = \pm 15$, *i.e.* 20 μm on the crystal, only two branches are seen to be strongly excited for each incident beam polarization. These are the ones excited also in the two-beam case, namely branches 1 and 4 ($\xi < 0$) and branches 1 and 5 ($\xi > 0$) for the σ polarization, and branches 2 and 3 ($\xi < 0$) and branches 4 and 6 ($\xi > 0$) for the π polarization of the incident beam. Although the excitation coefficients converge relatively rapidly towards the two-beam value for increasing ξ, the distances between the dispersion surface branches have a slower variation (Fig. 3). One may consequently expect the three-beam effect to be most easily observed in the displacement of the fringe positions rather than in the variation in the intensity.

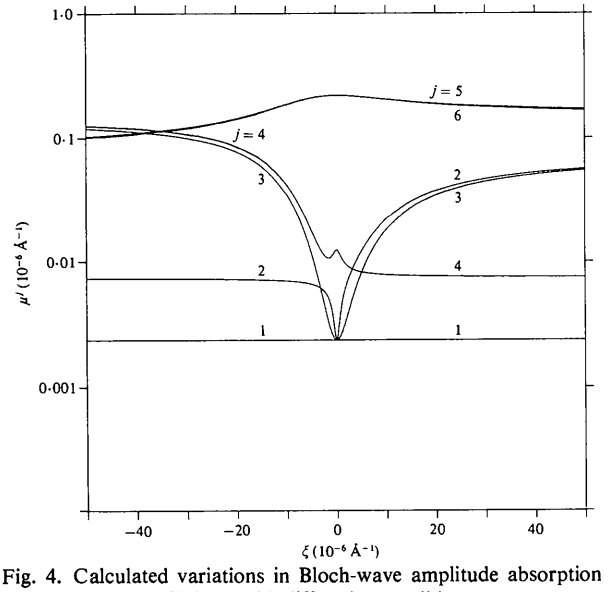

Fig. 4. Calculated variations in Bloch-wave amplitude absorption coefficients with diffraction condition.

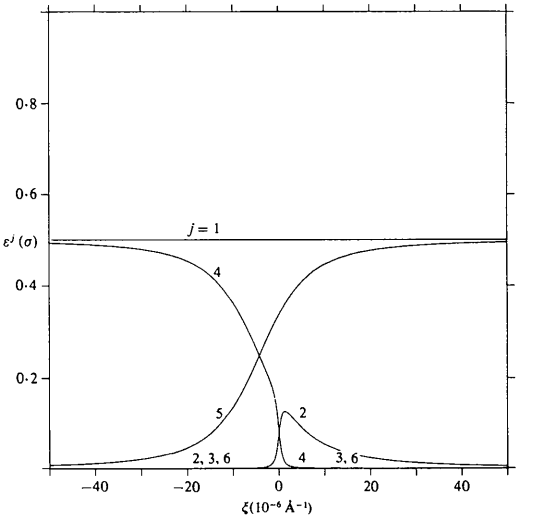

Fig. 5. Calculated excitation coefficient variation with diffraction condition. σ polarization.

Typical variations in excitation coefficients near gap positions are seen from the $|D^4_{0\sigma}|^2$ and $|D^5_{0\sigma}|^2$ curves near $\xi = 0$ in Fig. 5. The extent of the area with a rapid variation is determined by the gap width between the branches 4 and 5 located at $\xi = -4$ in Fig. 3. This dependence is also demonstrated in Fig. 6 where the variation of branches 3 and 6 can be ascribed to the corresponding large gap in Fig. 3. The coefficients of branches 2 and 4 on the other hand have clearly a more rapid variation with ξ. This is due to the narrow gap between branches 2 and 4 which results from the small σ, π coupling terms in (4).

The calculated intensity variations in the $2\bar{2}0$ *Pendellösung* pattern as a function of thickness and ξ are shown in Fig. 7. The ξ direction corresponds to the vertical direction of constant crystal thickness, and 1 mm in this direction on the plate represents 1280 ξ units in the experimental set-up used. The intensity variation shown results from direct copying of a computer printout. For all ξ only one strong period occurs in addition to the well known fading period. In accordance with the discussion above this reflects the coupling between only two branches for each polarization mode.

For $\xi > 0$ the fringe position bends towards smaller thicknesses while for $\xi < 0$ the bending is in the opposite direction. As pointed out above this is due to the deviation of the three-beam gap from the corresponding gap in the two-beam case. The latter one depends linearly on the structure factor $F_{2\bar{2}0}$. We can hence define an effective structure factor for the three-beam case depending on the fringe shift or the corresponding size of the dispersion surface gap. In this case we obtain $F^{3\text{-beam}}_{2\bar{2}0}$ $(\xi > 0) > F_{2\bar{2}0}$ and $F^{3\text{-beam}}_{2\bar{2}0}$ $(\xi < 0) < F_{2\bar{2}0}$.

As for all three-beam cases in Si the product between the three structure factors involved is positive, *i.e.* $P = F_{2\bar{2}0}F_{02\bar{2}}F_{\bar{2}02} > 0$. Theoretically this product may be taken to be negative through sign shifts in the structure factors. The dispersion surface and fringe pattern calculated for the case $P < 0$ are shown in Figs. 8 and 9. A comparison between Fig. 3 and Fig. 8 shows the influence of the sign of P, which is in accordance with known previous results (Kambe, 1957; Gjønnes & Høier, 1969; Post, 1979), *i.e.* cases where $\xi > 0$ for $P > 0$ correspond to the cases where $\xi < 0$ for $P < 0$.

The calculations given in Fig. 9 show that the fringe bending for the $P < 0$ case is opposite to the one for $P > 0$. From the bending direction alone we can therefore determine the sign of P, in principle, without any

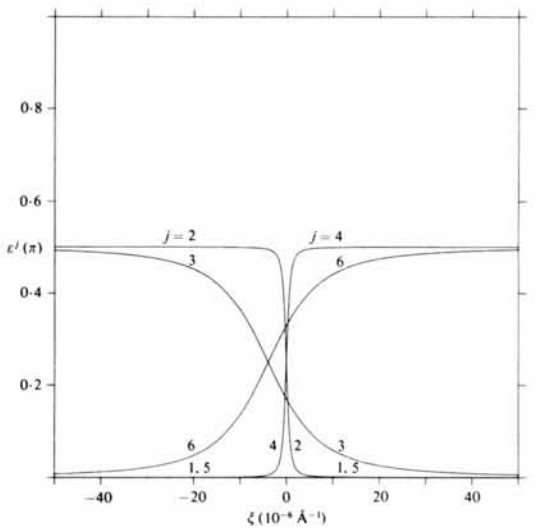

Fig. 6. Calculated excitation coefficient variation with diffraction condition. π polarization.

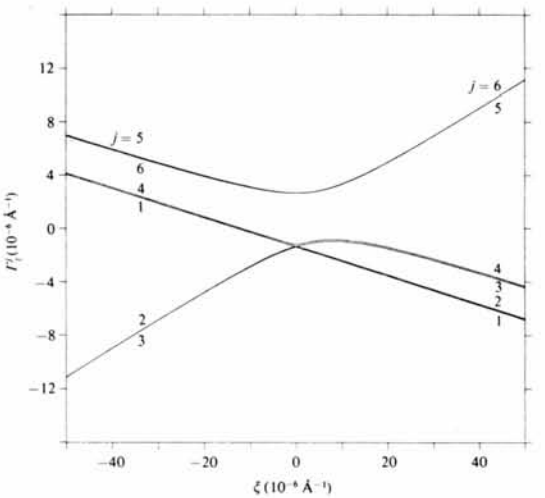

Fig. 8. Calculated dispersion surface. $F_h F_{-g} F_{g-h} < 0$.

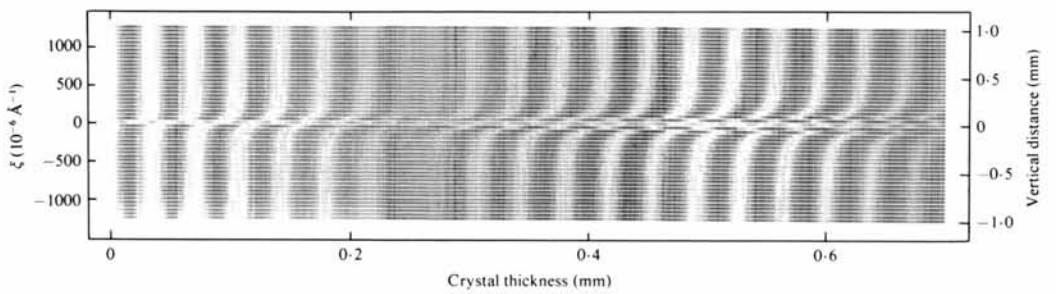

Fig. 7. Calculated variation in fringe contrast with thickness and diffraction condition. $F_h F_{-g} F_{g-h} > 0$. Mean absorption removed.

knowledge of the size of the structure factors involved. This is valid for the intensity contributions from each polarization mode independently, as shown in Fig. 10 for $P > 0$, and consequently also for their sum (Fig. 7). In conclusion, we can therefore neglect polarization effects in the interpretation and application of the three-beam effect discussed.

Experimental

The experiments have been done with a standard Lang camera using a Si crystal with a wedge angle of 2°, a Mo tube with point focus and L-4 plates. The effective focus size was 0·8 and 0·1 mm in the horizontal and vertical directions, respectively.

The experimental geometry corresponds to the one given in Fig. 2, *i.e.* the $(2\bar{2}0)$ planes are vertical and fulfil Bragg's law as in the usual two-beam set-up. The crystal has been rotated around the $(2\bar{2}0)$ plane normal bringing also the $(0\bar{2}2)$ planes into the Bragg position simultaneously.

Along a vertical line on the illuminated crystal area, *i.e.* the equal-thickness direction, each position on the crystal will now approximately correspond to one particular diffraction condition for the simultaneously excited beams. This is due to the relatively small focus height. As in the two-beam case, however, s_h varies negligibly with crystal height while s_g varies rapidly in the vertical direction.

The observed $2\bar{2}0$ *Pendellösung* fringes are shown in Fig. 11. The figure shows the usual two-beam variation in the far upper and far lower parts. Within a small area near the middle of the figure both the position and the intensity, however, deviate from the two-beam behaviour. This is the three-beam effect and the extent of the area where this effect is observable is seen to increase with crystal thickness.

The observed effect is asymmetric with respect to the position $s_g = 0$. Above this position in the figures $s_g > 0$ and the fringes are seen to be displaced towards smaller thicknesses while the bending is in the opposite direction below, *i.e.* for $s_g < 0$.

Near $s_g = 0$ a narrow line is observed, especially for larger thicknesses. This line has weak deficient contrast with smoothly varying intensity towards the fringes on the $s_g > 0$ side. On the other side, *i.e.* for small negative s_g, the line shows excess contrast especially between the fringes for larger thicknesses.

Discussion

Qualitatively the agreement between Fig. 11 and the calculated intensity distribution in Fig. 7 is very good. Both the observed direction of the fringe bending and the thickness dependence of the three-beam effect are

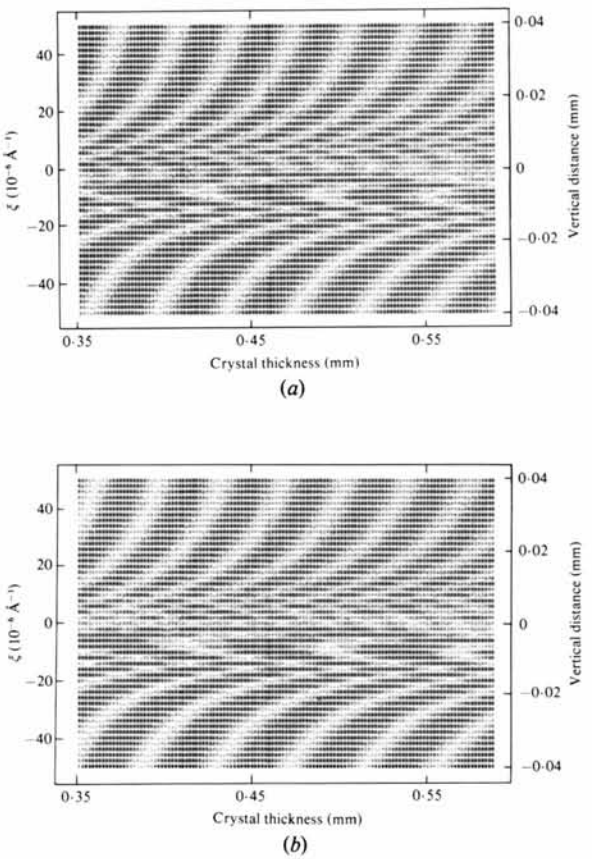

Fig. 10. Calculated variation in fringe contrast for (*a*) σ polarization and (*b*) π polarization of the incident beam. $P > 0$.

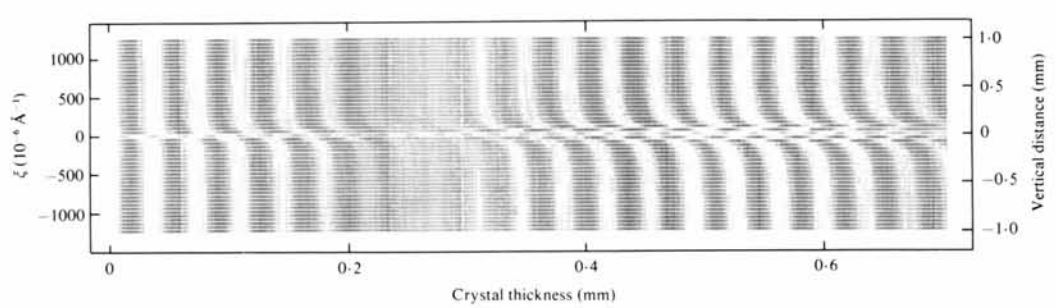

Fig. 9 Calculated variation in fringe contrast with thickness and diffraction condition. $F_h F_{-g} F_{g-h} < 0$. Absorption not included.

well reproduced by the calculations performed for a positive three-phase structure invariant.

Observable differences between theory and experiment can be seen, however, very close to the three-beam line. This fact may have several explanations. Firstly, the curvature of the dispersion surface is large near this position as seen from Fig. 3. Deviations from a plane-wave description may hence be essential. Secondly, we have an important integration effect which follows from the finite anode height. For the $0\bar{2}2$ beam the consequence is that each point on the crystal will diffract according to a range of incident beam directions. The local observed intensity therefore results from an integration over the corresponding range in s_g. Thirdly, the relative branch distances for $|\xi| \lesssim 100$ vary differently with ξ on the positive and negative side. The result is that the various terms in the σ and π contributions, Fig. 10, add up asymmetrically with respect to the sign of ξ resulting in an asymmetric intensity variation across the line.

The fringe distance in the upper and lower part of Fig. 10 may be interpreted in the standard two-beam way by means of the four parallel dispersion surface branches at large $|\xi|$ in Fig. 3. Here branch 1 or the branches 3 and 6 have pure σ or π components, respectively. Figs. 5 and 6 show that branches 4 and 2 approach pure σ and π character for increasing negative ξ, while the same variation is found for branches 5 and 4 for increasing positive ξ. The excitation of the branches 5 and 6 or 2 and 3 are negligible for large negative or large positive ξ, respectively. As we have no coupling between pure σ and pure π branches the well known two-beam intensity oscillations and fading effect arise at large $|\xi|$. For decreasing positive ξ and as long as the branches 2 and 3 are only weakly excited the two-beam argument can be used. The thickness fringe period, however, will depend on ξ through the deviation of $\Gamma^1 - \Gamma^5$ pure σ solution) and $\Gamma^4 - \Gamma^6$ (pure π solution) from the two-beam value. Neglecting fading we thus expect a single-period intensity oscillation depending on the size and sign of ξ. As the dispersion surface gaps, *e.g.* $\Gamma^1 - \Gamma^5$, are determined by the structure factor, we may in this case introduce an effective, three-beam structure factor $F_h^{3\text{-beam}}$. This quantity will be larger or smaller than the two-beam value, respectively, when ξ is negative or positive.

When ξ is less than approximately ± 30, more than four branches may be excited and some will have mixed σ and π character as can be seen from Figs. 5 and 6. This leads to an intensity oscillation with thickness which will no longer be represented by a single period, as several $(\Gamma^i - \Gamma^j)$ differences will contribute. The width of the area on the plate where this effect is expected to occur is very small. The effect is therefore not observed in Fig. 10 due to lack of sufficient experimental resolution.

The rotation of some of the field components with ξ should be noticed. This effect is especially clear for branch 4. With the polarization direction chosen in Fig. 2, D_0^4 is from Figs. 5 and 6 seen to rotate from almost pure σ to π within a change of 10 in ξ. This corresponds to a change in the diffraction condition of only approximately 1·5″.

Conclusions

A quantitative understanding of the variations in *Pendellösung* fringes has, as a rule, to be based on a spherical-wave description. However, as long as the focus is on a qualitative description of the intensity variations or on the fringe period in not too thin crystals, the simpler plane-wave treatment has demonstrated its applicability. This has previously been demonstrated for the determination of the size of structure factors with reasonable accuracy from two-beam experiments.

In the present studies one more beam has been introduced experimentally to see whether additional structural information may be obtained in that case. This depends on a reliable theoretical model for the effects utilized. It is found for the *Pendellösung* case that a sufficiently detailed qualitative understanding of three-beam effects may be obtained from a plane-wave description. Both the observed intensity variations and fringe bending have been reproduced theoretically. This fact may be ascribed to the directions of the normals of the contributing dispersion surface branches. These directions are so close to the corresponding two-beam directions for the ξ values of importance, that the usual spherical-wave interference arguments apply also in the present case.

The observed anomalies near three-beam positions may profitably be related to the dispersion surface. Here the corresponding gap distances depend on the deviation parameter of the third beam. The sign of this parameter determines whether the gap distance is larger

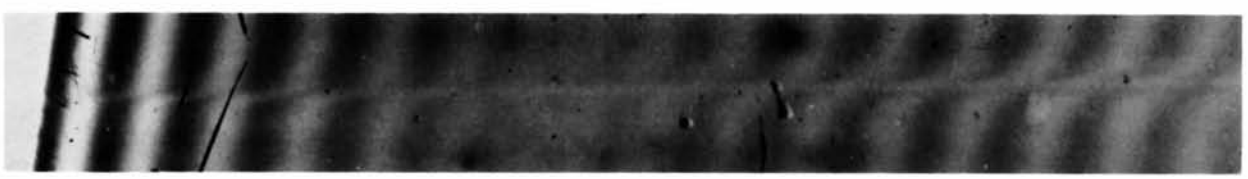

Fig. 11. Observed *Pendellösung* fringe contrast in the $2\bar{2}0$ beam for the 000, $2\bar{2}0$, $0\bar{2}2$ case in Si. Mo $K\alpha$. ×10·8.

or smaller than the corresponding two-beam gap. For a given sign of the deviation parameter, the direction of the fringe bending is found to depend on the sign of the product between the three structure factors involved in the three-beam calculations. This effect may thus be utilized to determine three-phase structure invariants experimentally. In structure work, however, the method may at the present stage of development only be applied in a limited number of cases as relatively large single crystals are needed.

To determine the branches which contribute most strongly to the intensity the calculations of excitation coefficients have proved to be essential. Only the four branches, which correspond to the ones in the two-beam case, are, through such calculations, found to be of importance. These branches contribute to the intensity oscillations in pairs corresponding to the σ and π components. The present calculations therefore show that polarization contributes in the usual way to the fading, but are not essential for the interpretation of the three-beam effects studied.

References

ALDRED, P. J. E. & HART, M. (1973*a*). *Proc. R. Soc. London Ser. A*, **332**, 223–238.

ALDRED, P. J. E. & HART, M. (1973*b*). *Proc. R. Soc. London Ser. A*, **332**, 239–254.

AZAROFF, L. V., KAPLOW, R., KATO, N., WEISS, R. J., WILSON, A. J. C. & YOUNG, R. A. (1974). *X-ray Diffraction*. New York: McGraw-Hill.

EWALD, P. P. & HENO, Y. (1968). *Acta Cryst.* A**24**, 1–15.

GJØNNES, J. & HØIER, R. (1969). *Acta Cryst.* A**25**, 595–602.

HART, M. & LANG, A. R. (1961). *Phys. Rev. Lett.* **7**, 120–121.

HILDEBRANDT, G. (1967). *Phys. Status Solidi*, **24**, 245–261.

HØIER, R. (1973). *Acta Cryst.* A**29**, 663–672.

HØIER, R., EKRANN, T. & AANESTAD, A. (1978). *Acta Cryst.* A**34**, S233.

JAMES, R. W. (1963). *Solid State Physics*, edited by F. SEITZ & D. TURNBULL, Vol. 15, pp. 55–220. New York: Academic Press.

JOKO, T. & FUKUHARA, A. (1967). *J. Phys. Soc. Jpn*, **22**, 597–604.

KAMBE, K. (1957). *J. Phys. Soc. Jpn*, **12**, 13–25.

KAMBE, K. & MOLIÈRE, K. (1970). *Advances in Structure Research by Diffraction Methods*, edited by R. BRILL & R. MASON, Vol. 3, pp. 53–100. Oxford: Pergamon Press.

KATO, N. (1968*a*). *J. Appl. Phys.* **39**, 2225–2230.

KATO, N. (1968*b*). *J. Appl. Phys.* **39**, 2231–2237.

KATSNELSON, A. A., IVERONOVA, V. I., BORODINA, T. I. & RUNOVA, T. K. (1975). *Phys. Status Solidi A*, **15**, K83–K86.

PETERS, G. & WILKINSON, J. H. (1970). *Numer. Math.* **16**, 181–204.

POST, B. (1977). *Phys. Rev. Lett.* **39**, 760–763.

POST, B. (1979). *Acta Cryst.* A**35**, 17–21.

POST, B., CHANG, S. L. & HUANG, T. C. (1977). *Acta Cryst.* A**33**, 90–97.

RENNINGER, M. (1937). *Z. Phys.* **106**, 141–176.

SACCOCIO, E. J. & ZAJAC, A. (1965). *Phys. Rev.* **139**, A255–A264.

TANEMURA, S. & KATO, N. (1972). *Acta Cryst.* A**28**, 69–80.

TERASAKI, O., WATANABE, D. & GJØNNES, J. (1979). *Acta Cryst.* A**35**, 895–900.

WADA, M. & KATO, N. (1977). *Acta Cryst.* A**33**, 161–168.

Acta Cryst. (1981). A**37**, 794–801

Diffraction by Crystals with Planar Domains

BY W. ADLHART

Institut für Kristallographie und Mineralogie, Theresienstrasse 41, *D*-8 *München* 2, *Federal Republic of Germany*

(*Received* 27 *January* 1981; *accepted* 9 *April* 1981)

Dedicated to Professor Dr H. Jagodzinski on his 65th birthday

Abstract

A general theory is developed for kinematical scattering by crystals with lamellar domains, having two equal lattice translations **b** and **c** which form a congruent plane of intergrowth. The domains differ in the lattice constant **a**, electron density distribution, and inter-domain distances. The size of the domains is described by arbitrary statistical distribution functions and the scattered intensity is calculated by forming the Patterson function and its Fourier transform. Examples with two types of domains are discussed.

0567-7394/81/060794-08$01.00

1. Introduction

A great number of electron microscopic and X-ray investigations deal with crystals with planar faults due